CHIMIA 2000, 54, No. 3

Chimia 54 (2000) 96–102

ISSN 0009–4293

Photochemistry of Hydrocarbon Radicals

Ingo Fischer*
Ruzicka Prize Winner 1999

Abstract: Hydrocarbon radicals are ideal model systems to understand the dynamics of chemical reactions. In addition they are of considerable importance in high-energy environments, such as combustion engines or hydrocarbon crackers. In order to understand their reactions, we deposit a known amount of energy in the radicals by laser excitation and observe the subsequent dynamics by two experimental methods, a) picosecond time-resolved photoelectron spectroscopy and b) nanosecond photoionization of hydrogen atoms, the major reaction product in many radical reactions.
Recent results for three radicals are summarized and discussed: allyl (C_3H_5), propargyl (C_3H_3), and ethyl (C_2H_5). We report the major reaction products, the pathways leading to these products, their rates of formation, and translational energy releases.

Keywords: Allyl · Photodissociation dynamics · Propargyl · Radicals · Time-resolved spectroscopyy

Ingo Fischer was born 1963 in Kassel, Germany. After receiving his chemistry Diploma in 1989 from the University of Bonn, he went to the Technische Universität München, to join the group of Vladimir E. Bondybey at the Institute for Physical Chemistry. In 1992 he obtained his Dr. rer. nat. with a thesis on high-resolution photoelectron spectroscopy. His research benefited from a collaboration with Klaus Müller-Dethlefs. From 1993 to 1995 he spent 20 months as a visiting scientist at the Steacie Institute for Molecular Sciences in Ottawa, Canada, working with Albert Stolow on ultrafast spectroscopy and wavepacket dynamics. In 1995 he joined the chemistry department of the ETH Zürich. He initiated an independent research program within the group of Peter Chen at the Laboratorium für Organische Chemie. After finishing his Habilitation, he was named Privatdozent in fall 1999. His current research interests comprise the areas of chemical dynamics, photochemistry and ultrafast spectroscopy.

*Correspondence: PD Dr. I. Fischer
Laboratorium für Organische Chemie
ETH Zentrum
Universitätstrasse 16
CH-8092 Zürich
Tel.: +41 1 632 44 89
Fax: +41 1 632 12 80
E-Mail: fischer@org.chem.ethz.ch
http://chen2.ethz.ch/ingo1.html

1. Introduction

How do chemical reactions proceed? This question, central to the field of chemical dynamics, fascinates almost every chemist. New spectroscopic methods permit us to investigate the microscopic details of reactions in increasing detail. We are interested in the chemical dynamics of organic radicals – a class of molecules largely unexplored, but of high importance. In this paper I will summarize some of our recent results on the dynamics and kinetics, as well as the photochemistry and photophysics of hydrocarbon radicals upon excitation with UV light. In contrast to thermal excitation, photon excitation has the advantage that a well-defined amount of energy can be deposited in the radical. Our emphasis is on small systems such as allyl (C_3H_5) [1][2], propargyl (C_3H_3) [3], and ethyl (C_2H_5) [4], depicted in Scheme 1.

1.1. *Motivation*

Our interest in hydrocarbon radicals originates from a number of properties of these compounds:

a) Radicals often possess low-lying excited electronic states with interesting couplings between them, making them ideal model compounds to study molecular behavior beyond the Born-Oppenheimer approximation (non-adiabatic effects).
b) Barriers to unimolecular reactions are often low, thus excitation with visible or near-ultraviolet light suffices to induce unimolecular reactions in these systems. The energetically and entropically most favorable reaction channel is often the loss of a hydrogen atom, because a closed-shell molecule is formed.
c) Since in many cases several products of the dissociation process are energetically close-lying, competing reaction channels exist. For example, in the case of both allyl and propargyl, loss of a hydrogen atom can lead to the formation of three different structural isomers with the composition C_3H_{n-1}.
d) Although the dynamics of radicals shows a complexity comparable to that of much larger molecules, they are small enough to be studied by the sophisticated methods of laser spectroscopy. To our mind this makes them ideal model systems to investigate chemical dynamics in general.

But hydrocarbon radicals are also of considerable chemical importance. We concentrate on systems that play a role in combustion processes or in hydrocarbon cracking. Both propargyl and allyl are considered in kinetic models to be important intermediates in the formation of polycyclic aromatic hydrocarbons and soot [5], in that an aromatic C_6 unit can form from two C_3 units in one bimolecular step

only. Understanding soot formation is an important problem, because of both the carcinogenic potential and the associated engine damage. The accuracy of kinetic models describing combustion systems depends on the rates for hydrogen loss or association [6].

Let us summarize the specific goals of our research program. We want to

- identify the products of unimolecular reactions of organic radicals,
- understand in detail the reaction pathways leading to those products,
- determine the timescales for the different steps involved in the reaction,
- obtain information on the distribution of excess energy on the product degrees of freedom.

2. Methods

2.1. *Experimental Techniques*

In order to achieve these goals, a combination of several experimental techniques with computational approaches is applied. Due to their high reactivity, radicals are best studied under isolated conditions. Therefore we perform all experiments in a molecular beam. A typical apparatus consists of a vacuum chamber with a mass or photoelectron spectrometer attached. The radicals are generated by a technique called supersonic jet flash pyrolysis [7]. In this method a suitable precursor, diluted in a rare gas, is expanded through a pulsed valve into the vacuum chamber. An electrically heated SiC tube is mounted onto this valve [8]. If the conditions (temperature, backing gas pressure, length and diameter of the SiC tube) are properly chosen, only the thermochemically weakest bond is cleaved and the radical of interest is generated in a clean manner. Scheme 1 shows some particularly efficient ways of generating allyl, ethyl and propargyl. The pyrolysis temperature necessary to produce allyl is around 800 °C, but temperatures up to 2000 °C are possible. Number densities of up to 10^{14} /cm^3 can be achieved at the nozzle exit. Upon expansion into the vacuum a supersonic beam is formed, leading to substantial cooling of the radicals.

The two spectroscopic techniques most important to us are a) time-resolved photoelectron spectroscopy (TR-PES) and b) time- and frequency-resolved multiphoton ionization (MPI) of hydrogen atoms. Instead of presenting the details of the setup, only a schematic representation of the physical principles will be given.

We monitor the primary photophysical events directly after photon absorption by picosecond time-resolved pump-probe photoelectron spectroscopy with a time resolution of around 2 ps [1]. Over the last decade short-pulse pump-probe spectroscopy evolved into a powerful method for investigating gas-phase dynamics [9][10]. This was recognized recently by the award of the 1999 Nobel prize to Prof. Zewail for his contributions to the field (see the article by M. Chergui in this issue). The principles of such an experiment are depicted in Fig. 1. In the first step the pump-laser transfers the molecule from the initial state |i> to an excited electronic state |j>, which evolves in time. This evolution can be bound motion (vibration or rotation), photophysical (non-radiative) processes, or a chemical reaction, like isomerization or dissociation. After a certain time delay a second laser, the probe, excites the molecule to a final state |k>, which serves as a template of the dynamical evolution. A whole scan is performed by monitoring the probe signal as a function of the time delay between the two laser pulses. Information on the fate of the initially pumped intermediate state can be extracted from the change in the probe signal with time. There are several different probe techniques which can be distinguished according to the chosen final state. For example, the probe laser can excite the molecule of interest (or possible reaction products) to a higher-lying electronic state and collect the laser-induced fluorescence from this state as a function of time delay. This is the method originally implemented by the Zewail group [11]. Alternatively, we use the ground state of the ion as the final state [12][13]. Here either the mass or the photoelectron spectrum is recorded as a func-

Scheme 1: Several ways to generate radicals by supersonic jet flash photolysis.

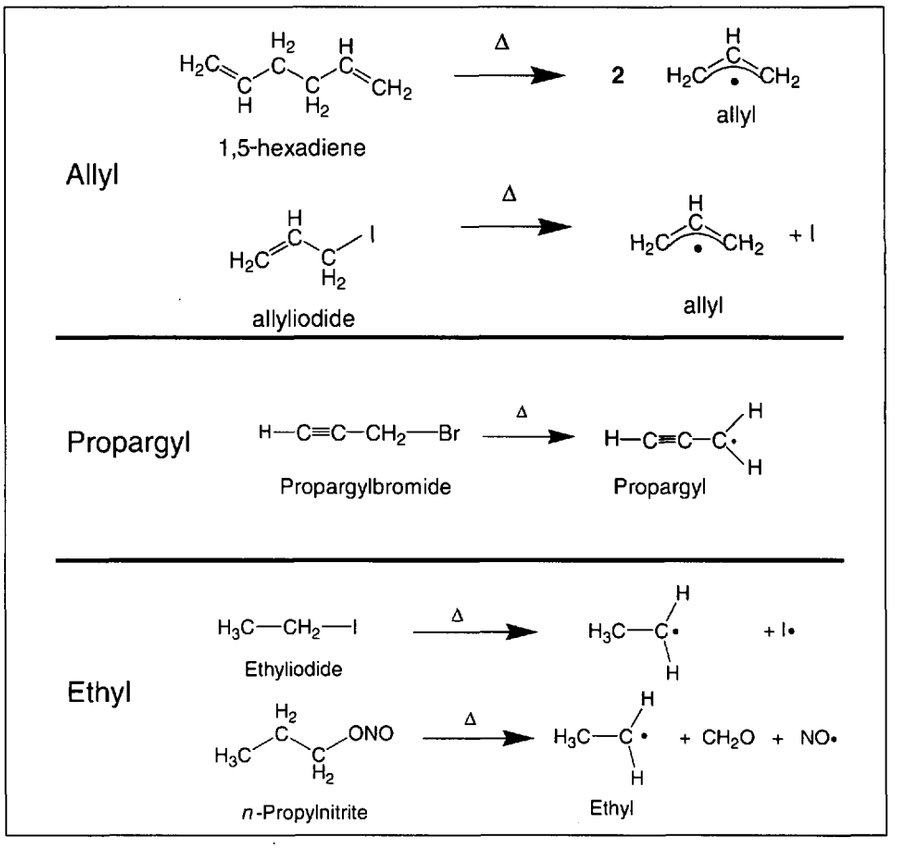

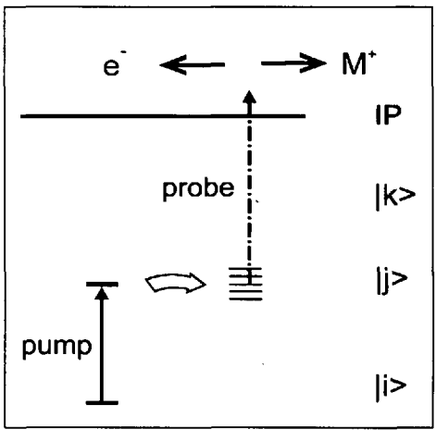

Fig. 1. In our picosecond time-resolved pump-probe experiments molecules are initially pumped to an excited electronic state. The dynamical evolution of this state is then monitored in the probe-step by ionizing the molecule and recording either the ion (mass) or the electron signal as a function of time.

tion of time. In the case of radicals this approach is particularly advantageous, because a) most radicals do not fluoresce, and b) because charged-particle detection is more sensitive than photon detection; a particular advantage when species are studied that can only be generated at small number densities.

The dissociation reactions themselves proceed on a nanosecond timescale. We investigate them by multi-photon ionization (MPI) of hydrogen atoms [14], an extremely sensitive detection technique. The principles of the technique are illustrated on the right-hand side of Fig. 2 (note that nanosecond-lasers are employed in this experiment). A first laser excites the radical of interest into an excited electronic state in the UV. As will be shown below, these states quickly decay by internal conversion to the ground state, forming vibrationally hot radicals. Thus electronic excitation is employed to deposit a fixed amount of thermal energy in the radical. The energy suffices to overcome the barrier to dissociation into a hydrogen atom and a molecular fragment. The H atom is then ionized by a second laser *via* the 1s–2p Lyman-α transition. Due to the high absorption cross section of this transition, H atom detection is far more sensitive than detection of the corresponding molecular fragment. In practice, a tunable laser operated around 365 nm is focussed into a cell filled with 200 mbar of Kr, generating VUV light around 121.6 nm. The H atoms are excited to the 2p state by the VUV photons, ionized by the residual 365 nm light, and detected in a time-of-flight mass spectrometer attached to our apparatus. If the relative time between the two lasers is varied, similar to the short-pulse experiment mentioned above, the rate of appearance of H atoms (and thus the reaction rate) can be monitored. In addition, two more parameters can be changed, the excitation wavelength, giving us control over the total energy deposited in the radical, and the detection wavelength, which permits the profile of the hydrogen absorption line (Doppler profile) to be recorded. As will be discussed below, information on the product energy distribution can be extracted from the Doppler profile.

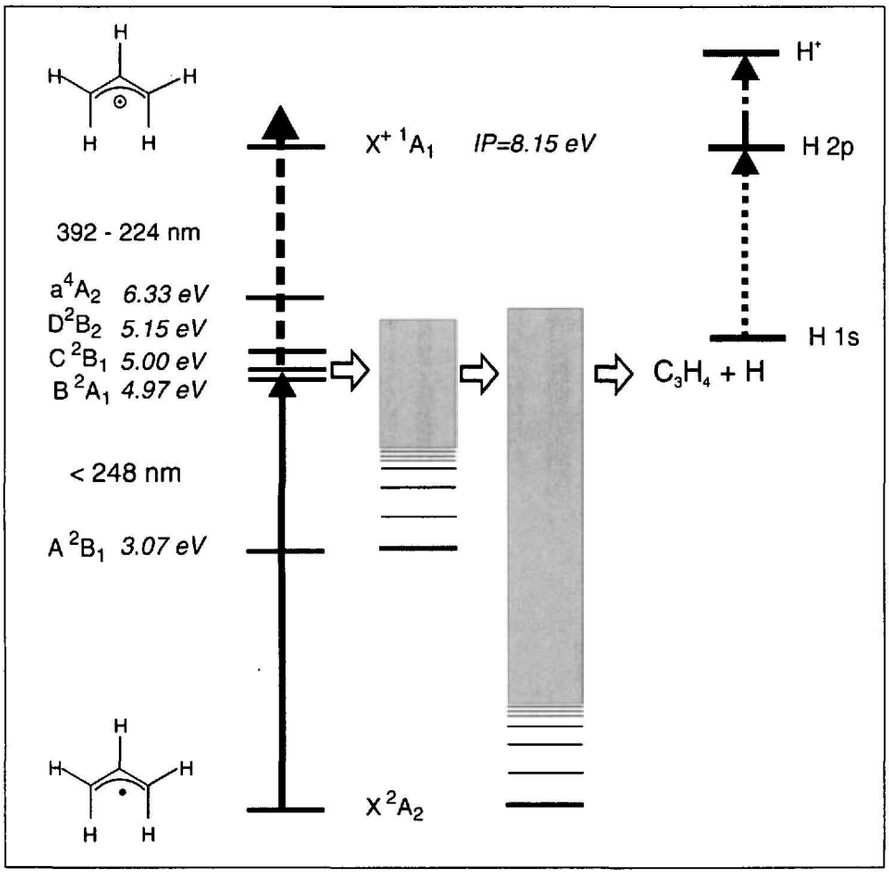

Fig. 2. Location of the electronic states in the allyl radical. The lifetime of the laser-excited UV bands (full arrow) is probed by ionization (dashed arrow). The bands decay in a two-step process *via* the intermediate A-state. Since electronic energy is converted to internal energy, allyl can overcome the barrier to dissociation into a molecular fragment and H atoms. The H is ionized *via* the 1s–2p resonance (dotted and dash-dot arrows); an extremely sensitive detection scheme.

2.2. *Theory*

We interpret the dissociation process within the framework of statistical theories of chemical reactions, in particular RRKM (Rice-Ramsperger-Kassel-Marcus) theory [15]. In RRKM the rate of a chemical reaction as a function of energy, $k(E)$ is described by the formula

$$k(E) = \frac{N^{\#}(E - E_0)}{h\rho(E)} \quad (1)$$

with $N^{\#}$ being the number of states at the transition state, E_0 the energy of the transition state, *i.e.* the barrier to dissociation, and ρ the density of states of the educt. Here ρ represents all possible ways to distribute energy over all degrees of freedom of the molecule, while $N^{\#}$ represents the number of possibilities that lead to a reaction. We obtain the barrier height, E_0, and the vibrational frequencies, necessary to calculate both $N^{\#}$ and $\rho(E)$ from *ab initio* calculation, using the Gaussian program package [16]. Typically we start with fourth-order perturbation theory (MP4) to calculate the reaction coordinate, to determine the stationary points, and to calculate the frequencies at these points. Subsequently more accurate coupled-cluster calculations are performed to improve the energies at the stationary points and get more accurate activation barriers.

3. Results

3.1. *Allyl*

Thanks to our work, allyl is now the best understood hydrocarbon radical. Here it will serve as a model system to illustrate our approach. The sequence of its electronic states is depicted in Fig. 2. While the structure of the $^2A_2$ ground state is well characterized by IR laser spectroscopy [17], much less is known about the first electronically excited $A\,^2B_1$ state around 3 eV. Although we recently started to investigate this state as well [18], most of our effort was dedicated to the UV band system around 5 eV, consisting of the $B\,^2A_1$, $C\,^2B_1$ and $D\,^2B_2$ states. Note that the first quartet state lies above the UV bands, a situation quite typical for many radicals. MPI investigations yielded a number of vibronic bands between 250 and 238 nm, some of them at least partially rotationally resolved [19]. However, the absence of fluorescence and the relatively sharp cut-off in the MPI spectrum at 238 nm indicate a fast decay of these states. In older theoretical work an excited-state photocycliza-

tion was proposed [20]. More recent resonance Raman investigations were found to be in agreement with this [21].

A typical time-resolved photoelectron spectrum [1] is depicted in Fig. 3. Here the pump laser excited allyl into the origin of the C-state at 248.1 nm. In the probe step, allyl was ionized by a second laser pulse around 274 nm and the photoelectrons formed upon ionization were detected. One axis represents the relative time delay between the two laser pulses, while the other axis gives the photoelectron spectrum for each time. Two different signals can be recognized: A time-independent one, around 1.8 eV electron kinetic energy, and a second, time-dependent one, at 1.37 eV. While the constant signal constitutes a time-independent background due to absorption of two pump photons, the time-dependent one reflects the population of the C-state. Initially, at negative time delays, *i.e.* with the probe laser arriving in time before the pump laser, the signal is absent. It appears as soon as the two lasers are overlapped in time and then decays monoexponentially with a time constant $\tau = 15$ ps. The lifetimes τ for all states between 250 and 238 nm were found to range from 20 ps (B-state origin) down to 9 ps. In a series of experiments, internal conversion (IC) to the electronic ground state was identified to be the major decay channel and not excited state photocyclization. The decay proceeds in a stepwise fashion, as indicated in Fig. 2. The UV states initially decay to the lower-lying A $^2B_1$ state and from there to the X $^2A_2$ electronic ground state. This interpretation was based on two observations [18]: a) Experiments on the fully deuterated allyl, C_3D_5, yielded an increase in lifetime by a factor of 4, indicating IC dominated by Franck-Condon factors instead of density of states [22], and thus to the nearest state. b) In *ab initio* calculations we identified a conical intersection between the A $^2B_1$ and the X $^2A_2$ states at a CCC bending angle of around 100°. Due to the correspondence between the allyl A-state and the cyclopropyl ground state as well as the allyl ground state and the cyclopropyl A-state, the curves cross along the coordinate to cyclization. Thus the measured time constants of 20 ps and less reflect the internal conversion from the UV bands to the A-state. Once allyl is on the A-state surface it decays to the ground state through the conical intersection presumably on a sub-picosecond timescale not resolvable by our experimental setup. Note that allyl is exceptional since the first excited A-state has a shorter lifetime than the higher states!

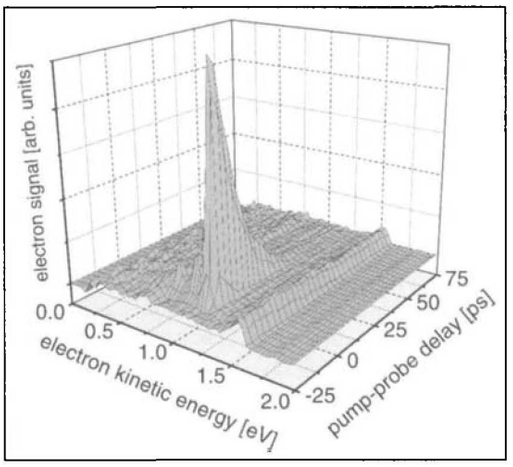

Fig. 3. Typical time-resolved photoelectron spectrum (TR-PES) from the C-state origin of allyl. From the time-dependent signal a decay constant of 15 ps can be extracted for this state. In addition, a time-independent signal, due to [1+1] process, is present at a different energy. The spectrum demonstrates the ability of TR-PES to detect time-dependent signals background-free.

Scheme 2: The different reaction channels for the allyl radical. In addition to direct loss of a hydrogen, allyl can undergo a hydrogen shift to 1- or 2-propenyl radical. Both species can lose hydrogen atoms to form either allene or propyne. A certain amount of C–C bond cleavage was also reported.

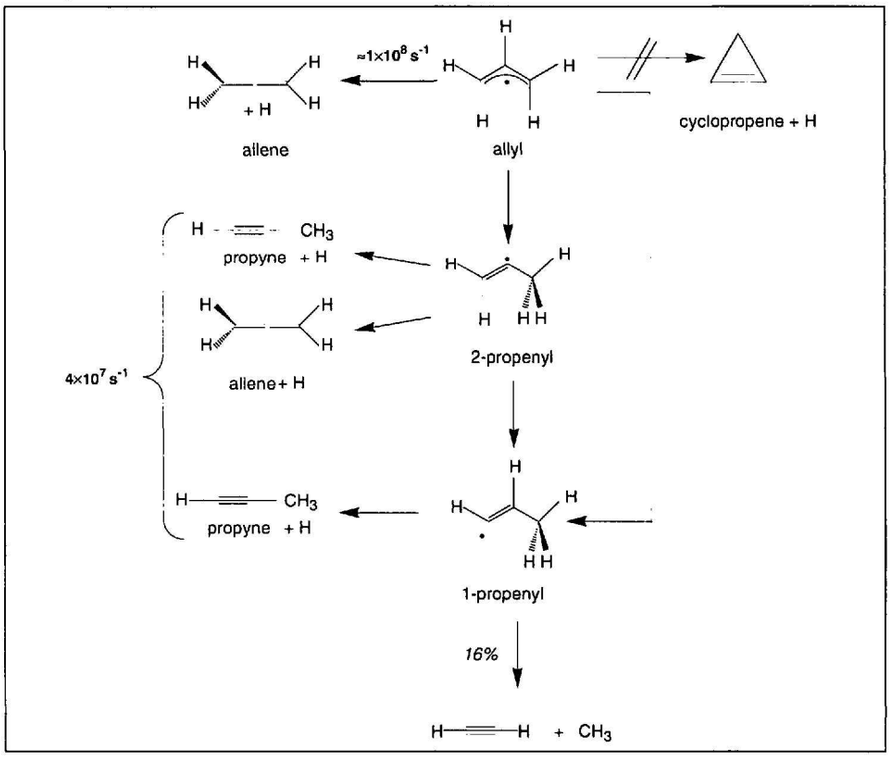

In this non-radiative decay, electronic energy is converted to internal energy, resulting in the formation of vibrationally hot allyl radicals with enough internal energy to overcome the barrier to dissociation to C_3H_4 and H, as indicated in Fig. 2. Three different C_3H_4 isomers can be formed in the dissociation process: allene, cyclopropene and propyne, all depicted in Scheme 2. The decisive experiments were carried out on the C_3HD_4 radical, with the terminal carbons selectively deuterated [2]. The laser used to detect H atoms was tuned over the 2p resonances of both H and D in order to monitor which bond is

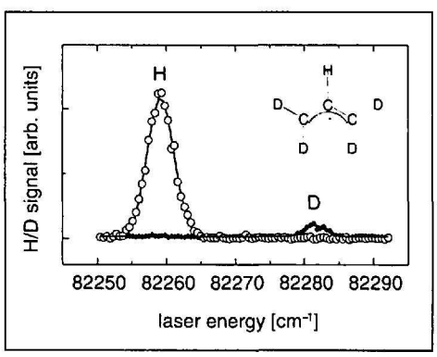

Fig. 4. Partially deuterated C_3HD_4 radicals lose predominately hydrogen, indicating that allene is the preferentially formed product.

preferentially cleaved. The resulting spectrum, depicted in Fig. 4, shows an intense H signal (open circles), about 10 times larger than the D signal (full diamonds). This demonstrates the preferential cleavage of the central C–H bond in allyl with subsequent formation of allene. Experiments on the inverse isotopomer, C_3H_4D, show preferential loss of D and thus confirm the results.

However, a certain amount of D loss is visible, indicating the presence of a second, minor reaction channel. *Ab initio* calculations of several possible reaction channels resulted in similar barriers for allene formation (63.3 kcal/mol) and hydrogen migration (66 kcal/mol) to 2-propenyl radical, but possibly also to 1-propenyl. Hydrogen loss from one of the propenyl radicals can yield both allene or propyne. As the H atoms will be scrambled in the H-migration process, no selectivity can be expected.

Scheme 2 summarizes what we have learned from our experiments. The dominant reaction channel is cleavage of the central C–H bond, leading to the formation of allene. Rate measurements yielded $k_1 \approx 10^8\ s^{-1}$ for this channel, in agreement with simple RRKM calculations. The second channel involves a hydrogen shift from allyl to one of several propenyl isomers. Although we can give a rate of $4\times10^7\ s^{-1}$ to the second channel, we cannot say conclusively to which of the possible reactions it has to be assigned. H loss proceeding through the 2-propenyl isomer seems to be most likely. However, the C–C bond cleavage in allyl was recently measured [23]. It was found that around 16% of the allyl cleaves into acetylene and methyl, a reaction that has to proceed from 1-propenyl and thus requires either two subsequent 1,2 H-shifts, or a 1,3 H-shift from allyl. This indicates a complex chemistry in this channel, with several contributing reactions. But the good news is that the dominant reaction channel, allene formation, is now well characterized. It should also be noted that there is no evidence for cyclopropene formation.

3.2. *Propargyl*

The 2-propynyl radical, commonly termed propargyl (C_3H_3), is presumably the most important hydrocarbon radical in combustion processes because dimerization of two propargyl units is considered to be the fastest route to benzene and phenyl formation in flames [24].

The second excited state of propargyl is also located around 250 nm. In contrast to allyl its UV spectrum, a broad absorption band ranging from 265 to 230 nm, is completely unstructured, presumably due to a very fast internal conversion to the ground state. Like in the allyl case, electronic energy is converted to internal energy, permitting us to investigate reactions on the ground-state surface [3]. As we lack the intermediate state selectivity of the allyl experiment, a clean generation of the radical is even more important. The mass spectra in Fig. 5 demonstrate how well this is possible for propargyl. The upper trace shows the spectrum with the pyrolysis source turned off. As visible, a signal due the precursor, C_3H_3Br (note the splitting due to the Br isotopes), appears upon ionization with 121.6 nm (10.2 eV) photons. A very small signal at m/e = 39 is present, but few hydrogen atoms are formed from the precursor. When the pyrolysis source is turned on (center trace) the signal from the precursor disappears almost completely, but an intense signal appears at the mass of propargyl, m/e = 39. No bromine atoms are detected, because of the ionization energy of 11.81 eV. When the excitation laser at 250 nm is turned in addition, the spectrum shown in the bottom trace is obtained. A strong signal at m/e = 1 appears, due to the dissociation of propargyl initiated by the excitation laser.

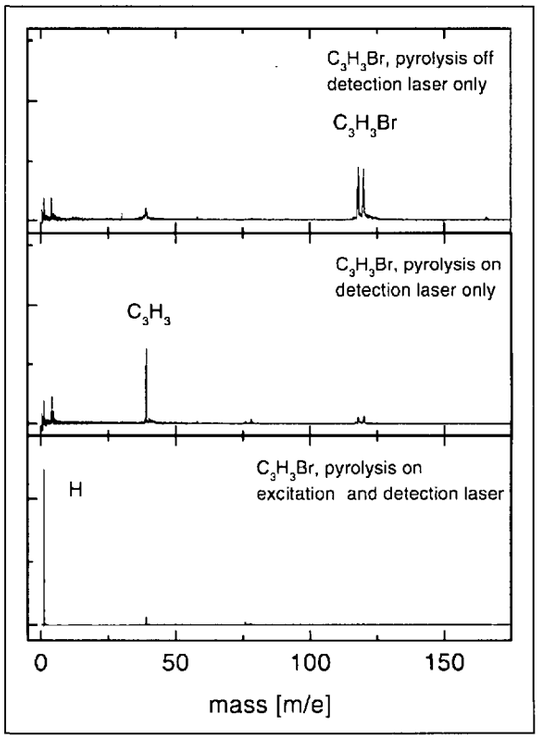

Fig. 5. Mass spectra recorded with the detection laser at 121.6 nm. With the pyrolysis source off (top trace), only little fragmentation of the precursor is evident. When the pyrolysis source is turned on (center trace), a signal due to propargyl appears, whereas the precursor signal disappears almost completely. When the excitation laser (242 nm) is turned on in addition (bottom trace), a strong hydrogen signal appears. Note that the y axis is compressed by a factor of ten in the bottom trace for ease of viewing.

Like in the allyl case, several different products of composition C_3H_2 can, in principle, be formed upon H loss from propargyl: cyclopropenylidene (c-C_3H_2), propadienylidene and propargylene, all depicted in Scheme 3. Since all possible products are carbenes, and thus reactive intermediates themselves, the barriers to reaction are relatively high. Note that the heat of formation is only well established for c-C_3H_2. As we carried out several of the experiments already described for allyl, we will only summarize the results. Again, experiments on partially deuterated propargyl, H_2CCCD, proved to be central to our understanding of the reaction mechanism. In contrast to allyl, complete isotopic scrambling was observed instead of regioselectivity. Scheme 3 indicates that formation of propadienylidene should be associated with cleavage of the acetylenic C–H bond (D loss in H_2CCCD), while propargylene formation should be accompanied by H loss from the CH_2 group. Both products should show regioselective H loss and are thus not in agreement with the observed scrambling.

Cyclopropenylidene, on the other hand, can be formed *via* two different processes, a two-step pathway (dashed line) and a three-step pathway (solid line) [25]. In the two-step pathway the H should be lost from the secondary carbon atom, and thus also be associated with regioselectivity. However, the three-step pathway proceeds *via* a 1,2 H-shift with subsequent cyclization. Here all hydrogens are equivalent and isotopic scrambling can be expected. Our data support c-C_3H_2 formation *via* the three-step pathway as the major reaction channel for H loss from propargyl.

The continuous absorption in the UV permits us to measure the rates for H loss as a function of excitation energy, given as

open circles in Fig. 6. For comparison, we performed RRKM calculations, assuming a reaction yielding c-C_3H_2 *via* the three-step pathway with a barrier of 90 kcal/mol. The educt (propargyl) frequencies were scaled by a factor of 0.71 to account for the effects of anharmonicity (open diamonds). As visible, experimental and calculated values agree within a factor of two, a good agreement for such a crude model, thus confirming the reaction mechanism proposed above. The deviation at the lowest excitation energy (marked by an arrow) is probably due to the small absorption cross section of propargyl at this wavelength, leading to a small signal and a rate associated with a large uncertainty.

3.3. *Ethyl*

Ethyl (C_2H_5) seems to be the simplest of the radicals discussed here. Loss of a H atom should yield ethene, among all possible products the thermochemically most stable one. Ethyl also has an unstructured absorption band around 250 nm, which corresponds to the first excited state of 3s Rydberg character. It can again be assumed that it decays rapidly by internal conversion to the ground state. Experiments on the partially deuterated CH_3CD_2 radicals [4] (Fig. 7) show exclusively a regioselective loss of hydrogen, in agreement with earlier measurements [26], suggesting a rather simple mechanism.

Again we measured reaction rates as a function of excess energy [4], depicted as an inset in Fig. 7. The measured values around 10^7 s^{-1} are consistent and fall approximately on a line. However, when compared to simple RRKM calculations, these rates turn out to be too slow by around four orders of magnitude, a rather surprising deviation. Possible explanations are the insufficient treatment of external and internal rotors in the RRKM calculations, or anharmonicity effects. Future experiments are planned in order to understand the deviation better.

Scheme 3: Of the three possible dissociation products of propargyl, cyclopropenylidene is the one formed preferentially. Our results indicate formation via a three-step pathway (solid line) rather than two-step pathway (dashed line).

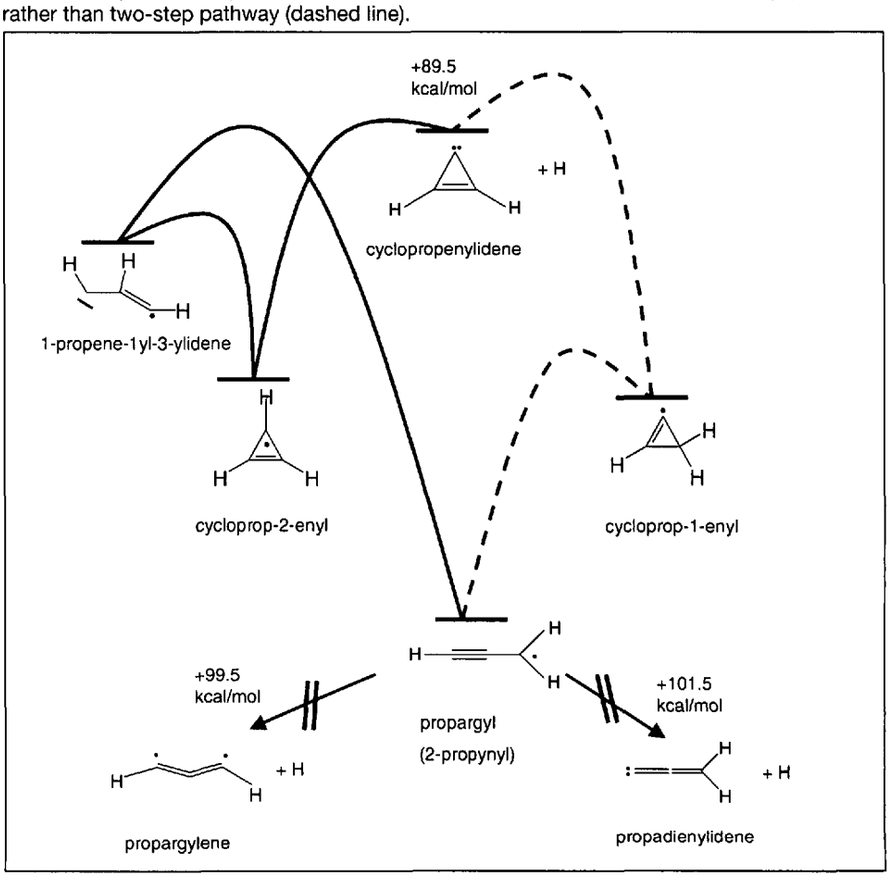

3.4. *Translational Energy Releases*

The Doppler profiles contain considerable information beyond just telling us whether H or D is lost from a given radical. When a molecule dissociates, a part of the excess energy is released as translational energy, E_T. Since the H atom is light, it will

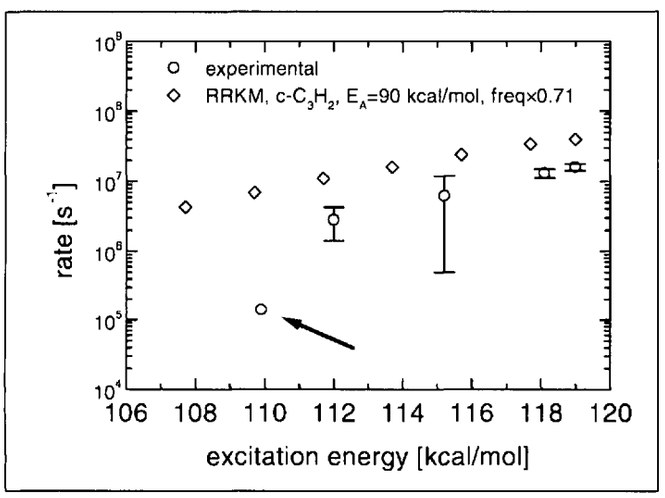

Fig. 6. The experimental rates for H loss from propargyl to c-C_3H_2 (open circles) can be well approximated by a simple RRKM model (open diamonds). The lowest energy data point, marked with an arrow, is probably unreliable, due to a poor signal-to-noise ratio in the experiment.

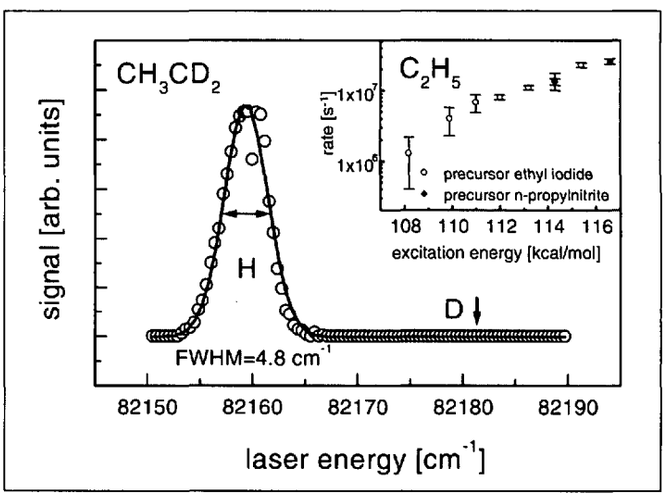

Fig. 7. H loss from ethyl occurs regioselectively as shown here for the CH_3CD_2 radical. Interestingly, the rates for H loss are four orders of magnitude slower than expected from simple statistical models (inset). Two different precursors were used in the kinetics studies: ethyl iodide (open circles) and *n*-propylnitrite (full diamonds).

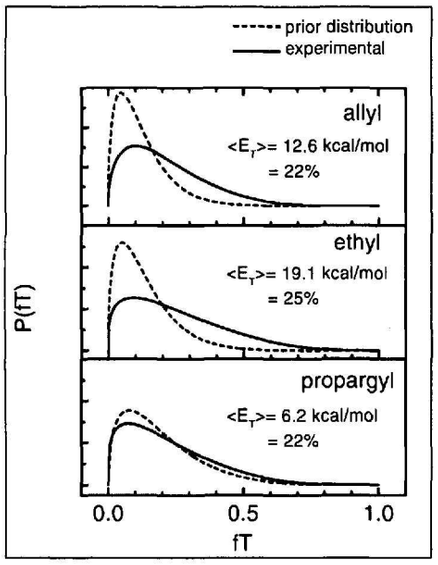

Fig. 8. Translational energy distributions derived from the H atom Doppler profiles (solid line) with a simple prior distribution (dotted line) given for comparison. For H loss from propargyl the agreement is very good, indicating a dissociation that is well described by statistical models. The deviations for H loss from ethyl and allyl can be explained by the reverse barrier, whose energy is preferentially released as translation.

carry away almost all of E_T and move out of the interaction region with considerable speed, leading to a broadening of the spectral line due to the Doppler effect. From this line broadening, a translational energy distribution $P(E_T)$, can be obtained, giving the probability of a certain translational energy release taking place in the experiment. For P we assumed the functional form

$$P(fT) = fT^a \times (1 - fT^b) \quad (2)$$

with fT being the fraction of excess energy (rather than the absolute amount) being released as translation, and a and b being adjustable parameters. The Doppler profile can be fitted from this distribution function by optimizing a and b *via* the inversion procedure given in the literature [27]. The translational energy distributions obtained for all three radicals are given as solid lines in Fig. 8, together with the expectation value, $<E_T>$, for the translational energy release. For all three radicals, between 20 and 25% of the excess energy is released as translation, within the range typical for statistical reactions. For comparison, the distribution derived from a simple statistical model, a prior distribution, is given for all radicals as a dotted line. For the reaction from propargyl leading to cyclopropenylidene, the measured and the prior distribution agree very well. For allyl and ethyl, the prior distribution peaks at smaller values of fT than the experimental function. This discrepancy is most likely due to the existence of a reverse barrier for the H loss that is not taken into account in a prior distribution. Interestingly, the computational results for the three-step reaction pathway from propargyl to c-C_3H_2 yielded a loose transition state with no reverse barrier for the rate-determining step, H loss from the cycloprop-2-enyl intermediate. Thus the analysis of the Doppler profiles and the associated translational energy distribution supports the interpretation derived above.

4. Summary and Conclusion

By combining a number of different experimental methods and supporting them by computation, we obtained a rather complete picture of the reactivity of three hydrocarbon radicals, each constituting a limiting case for chemical dynamics: From allyl several different products can be formed *via* relatively low barriers. Hydrogen loss from propargyl can also lead to different products, but *via* relatively high barriers. Finally, dissociation of ethyl leads to one product *via* a low barrier.

We showed that the UV bands of allyl decay within 20 ps by internal conversion *via* the lower-lying A-state. We identified a conical intersection between the A- and the ground state, indicating a very fast decay of the A-state. Allyl subsequently dissociates on the ground-state surface, the dominant reaction product being allene. Hydrogen loss from propargyl leads to the formation of cyclopropenylidene in a three-step pathway. Both reactions can be well described by statistical models. For ethyl, however, we found reaction rates four orders of magnitude slower than expected from simple statistical models, indicating that further work is necessary to understand its dynamics.

Acknowledgements

I am indebted to a number of excellent students who contributed to the various projects: H.-J. Deyerl (now at UC San Diego), T. Schultz (now at the NRC in Ottawa), and T. Gilbert, as well as a postdoc, T. Grebner. I would also like to acknowledge Prof. P. Chen for his continuous and generous support, as well as for many stimulating and helpful discussions. Financial support came from the Schweizerische Nationalfonds and the ETH Zürich. I would like to thank Dr. James S. Clarke for carefully reading the manuscript.

Received: January 21, 2000

[1] T. Schultz, I. Fischer, *J. Chem. Phys.* **1998**, *109*, 5812.
[2] H.-J. Deyerl, I. Fischer, P. Chen, *J. Chem. Phys.* **1999**, *110*, 1450.
[3] H.-J. Deyerl, I. Fischer, P. Chen, *J. Chem. Phys.* **1999**, *111*, 3441.
[4] T. Gilbert, T.L. Grebner, I. Fischer, P. Chen, *J. Chem. Phys.* **1999**, *110*, 5485.
[5] N.M. Marinov, M.J. Castaldi, C.F. Melius, W. Tsang, *Combuct. Sci. Technol.* **1997**, *128*, 295.
[6] J.A. Miller, R.J. Kee, C.K. Westbrook, *Annu. Rev. Phys. Chem.* **1990**, *41*, 345.
[7] P. Chen, in 'Unimolecular and Bimolecular Reaction Dynamics', Eds. C.Y. Ng, T. Baer, I. Powis, Wiley, New York, **1994**.
[8] D.W. Kohn, H. Clauberg, P. Chen, *Rev. Sci. Instrum.* **1992**, *63*, 4003.
[9] 'Femtosecond Chemistry', Eds. J. Manz, L. Wöste, VCH, Weinheim, **1995**.
[10] 'Femtochemistry', Ed. M. Chergui, World Scientific, Singapore, **1996**.
[11] A.H. Zewail, 'Femtochemistry', vol. I and 2, World Scientific, Singapore, **1994**.
[12] T. Baumert, M. Grosser, R. Thalweiser, G. Gerber, *Phys. Rev. Lett.* **1991**, *67*, 3753.
[13] I. Fischer, M.J.J. Vrakking, D.M. Villeneuve, A. Stolow, *Chem. Phys.* **1996**, *207*, 331.
[14] H. Zacharias, H. Rottke, J. Danon, K.-H. Welge, *Opt. Commun.* **1981**, *37*, 15.
[15] T. Baer, W.L. Hase, 'Unimolecular Reaction Dynamics', Oxford University Press, New York, **1996**.
[16] M.J. Frisch, G.W. Trucks, H.B. Schlegel, P.M.W. Gill, B.G. Johnson, M.A. Robb, J.R. Cheeseman, T.Keith, G.A. Petersson, J.A. Montgomery, K. Raghavachari, M.A. Al-Laham, V.G. Zakrzewski, J.V. Ortiz, J.B. Foresman, J. Cioslowski, B.B. Stefanov, A. Nanayakkara, M. Challacombe, C.Y. Peng, P.Y. Ayala, W. Chen, M.W. Wong, J.L. Andres, E.S. Replogle, R. Gomperts, R.L. Martin, D.J. Fox, J.S. Binkley, D.J. Defrees, J. Baker, J.P. Stewart, M. Head-Gordon, C. Gonzalez, J.A. Pople, Gaussian 94, Gaussian Inc., Pittsburgh, PA, **1995**.
[17] E. Hirota, C. Yamada, M. Okunishi, *J. Chem. Phys.* **1992**, *97*, 2963.
[18] T. Schultz, J.S. Clarke, H.-J. Deyerl, T. Gilbert, I. Fischer, *Faraday Discuss.* **2000**, *115*, in press.
[19] J.A. Blush, D.W. Minsek, P. Chen, *J. Phys. Chem.* **1992**, *96*, 10150.
[20] P. Merlet, S.D. Peyerimhoff, R.J. Buenker, S. Shih, *J. Am. Chem. Soc.* **1974**, *96*, 959.
[21] J.D. Getty, M.J. Burmeister, S.G. Westre, P.B. Kelly, *J. Am. Chem. Soc.* **1991**, *113*, 801.
[22] M. Bixon, J. Jortner, *J. Chem. Phys.* **1968**, *48*, 715.
[23] D. Stranges, M. Stemmler, X. Yang, J.D. Chesko, A.G. Suits, Y.T. Lee, *J. Chem. Phys.* **1998**, *109*, 5372.
[24] J.A. Miller, C.F. Melius, *Combustion and Flame* **1992**, *91*, 21.
[25] L. Vereecken, K. Pierloot, J. Peeters, *J. Chem. Phys.* **1998**, *108*, 1068.
[26] J.L. Brum, S. Desmukh, B. Koplitz, *J. Chem. Phys.* **1990**, *93*, 7504.
[27] Y. He, J. Pochert, M. Quack, R. Ranz, G. Seyfang, *Faraday Discuss.* **1995**, *102*, 275.